Thermal cracking characteristics and mechanism of sandstone after high-temperature treatment

Weijing Xiao[1, 2], Guo Yu[3], Haitao Li[3], Dongming Zhang[1, 2✉], Shujian Li[2], Beichen Yu[1, 2], Dongwei Li[1, 2]

[1] State Key Laboratory of Coal Mine Disaster Dynamics and Control, Chongqing University, Chongqing 400044, China.

[2] School of Resources and Safety Engineering, Chongqing University, Chongqing 400044, China.

[3] Exploration and Development Research Institute, PetroChina Southwest Oil and Gas Field Company, Chengdu, Sichuan 610041, China.

✉ **Corresponding author at:** State Key Laboratory of Coal Mine Disaster Dynamics and Control, Chongqing University, Chongqing 400044, China

Corresponding author: Dongming Zhang

Email: zhangdm@cqu.edu.cn

Abstract: To study the thermal cracking characteristics and mechanism of sandstone after high-temperature treatment, the pore size distribution and micromorphology of sandstone were observed by nuclear magnetic resonance and scanning electron microscopy. Then, based on the Weibull distribution theory, a thermal elastic mechanical model of random heterogeneous rock was established for the rock unit, the thermal stress distribution characteristics of sandstone were analysed, and the thermal fracture mechanism of rock was discussed. The results show that the porosities of the samples increased with increasing temperature, and the proportion of large pores increased significantly when exceeded 400 °C. Particularly when reached 1000 °C, thermal cracking was distributed in a complex network. Additionally, different rock units are in different thermal stress states, which leads to the regional differences in the distribution of rock thermal fracture. When exceeded 400 °C, there were obvious thermal cracks near the outer edge that weakened the mechanical properties of rock.

Keywords: high-temperature treatment; thermal cracking; scanning electron microscopy; thermal stress

Nomenclature

α	thermal expansion coefficient
α_0, m	distribution parameter
σ_{ij}	stress tensor
σ_r	radial thermal stress
σ_θ	circumferential thermal stress

ε_{ii} strain tensor
λ, G Lame constants
μ Poisson's ratio
$\tau_{r\theta}$ tangential thermal stress
C_1, C_2 integral constants
E Young's modulus
F_i external force
$F(r)$ cumulative distribution function of Weibull distribution
H(x) hyperbolic tangent function
K bulk deformation modulus
NMR nuclear magnetic resonance
R radius of sample
SEM scanning electron microscopy
T_2 transverse relaxation time
T_{2b} transverse relaxation time of free fluid
T_{2s} transverse relaxation time of fluid caused by surface relaxation
T_{2d} transverse relaxation time caused by diffusion relaxation in gradient magnetic field
T_0 center temperature of the sample at room temperature
T_a target temperature of the sample
T temperature
u, v displacement vector of a particle

1 Introduction

Rock is the main research object in underground space engineering [1-4]. With the continuous development of large-scale rock engineering, such as in deep resource development [5], oil and gas resources and deep storage of nuclear waste [6, 7], rock is subjected to complex geological environments, such as high stress, high osmotic pressure and high temperature, in many projects [8]. For example, in the process of underground coal gasification mining (UCG), the highest temperature of the gasification channel reaches 1200 °C [9]. Under the influence of such high temperatures, the stability of the rock surrounding the gasification channel is the main factor affecting safe mining. In underground nuclear waste storage, high-level nuclear waste will continue to release considerable heat during the decay process and warm the rock surrounding the nuclear waste repository. The cracks generated by high temperature may induce the leakage of nuclear waste and ultimately affect the stability of the nuclear waste repository [10, 11]. Therefore, the physical and mechanical properties of rock under high temperature are one of the most important research areas in the field of rock mechanics [12-14].

In view of the evolution law for rock physical and mechanical properties under the influence of high temperature, scholars have carried out many experimental studies and obtained fruitful research results [15-17]. Qin et al. carried out laboratory mechanical tests on granite treated at different temperatures [15]. The results showed that 400 °C is the critical temperature at which the mechanical properties of rock are affected. When the temperature exceeded 400 °C, the rock softened gradually with increasing temperature. Xiao et al. carried out uniaxial compression tests on sandstone treated at 25~1000 °C, and the results showed that the rock strength at the 400 °C critical temperature first increased and then decreased with increasing temperature, and the degree of rock failure increased obviously when the temperature exceeded 800 °C [16]. A uniaxial compressive test of sandstone was carried out by Ranjith at various temperatures ranging between 25 and 950 °C. The research results show that the strength and elastic modulus of sandstone gradually increased with increasing temperature in the range 25~500 °C and gradually decreased with increasing temperature when the temperature exceeded 500 °C [18]. In addition, to study the mechanical properties of sandstone treated at different temperatures, Gautam et al. [19], Zhu et al. [20] and Rao et al. [21] carried out laboratory mechanical tests on sandstone treated at different temperatures. The above research results showed that temperature can significantly affect the macromechanics of rock, which has been widely recognized by experts and scholars in the field of rock mechanics. At the same time, under the influence of temperature, the microstructure and void distribution of rock also change significantly. This is because the rock is mainly composed of crystalline minerals, mineral boundaries, pores and fissures. When the temperature rises, physical and chemical changes such as hot melting, thermal fracture and high-temperature phase transition occur in the rock microstructure, resulting in a change in rock micromechanics [22, 23]. Zhang et al. studied the voidage characteristics of sandstone treated at different temperatures (25 °C to 600 °C), and the results showed that the voidage diameter of sandstone ranged from 0.7 μm to 3 μm. When the temperature exceeded 400 °C, the cumulative voidage volume of sandstone changed dramatically [24]. Tripathi et al. carried out experimental research on the microstructural characteristics of sandstone under the influence of temperature, and the research results showed that the thermal fracture crack density of sandstone microstructure increased significantly at 300~500 °C [25]. To study the influence of temperature on the structure of pores and fractures in sandstone, the experimental study of Jin et al. on temperature-treated sandstone involved the use of SEM and NMR characterization, and the results showed that temperature promoted the development of rock voids and cracks, especially when the temperature exceeded 500 °C, and the number of sandstone voids and thermal fracture cracks increased significantly [26]. At the meso level, rock is a heterogeneous body composed of different mineral particles. Each mineral particle has a different expansion coefficient, which leads to different deformations under the influence of temperature. However, there is a continuum, so each mineral particle in rock cannot deform completely according to its own expansion coefficient. Therefore, there are constraints operating between mineral particles, resulting in thermal stress [27-29]. Thermal stress is the main factor inducing thermal cracking, and the distribution characteristics of thermal cracks are of great significance to the stability of rock engineering. Therefore, it is necessary to investigate the thermal cracking characteristics and mechanism of rock under the influence of temperature, and there are few reports on this aspect.

Based on this, the pore size distribution, micromorphology and thermal crack distribution of sandstone treated at different temperatures were analysed by nuclear magnetic resonance (NMR) and scanning electron microscopy (SEM). Then, considering the random heterogeneity of rock particles, a random medium thermoelastic model was constructed. Based on the Weibull distribution, the distribution characteristics of thermal stress in rock samples under different temperatures were analysed, and the thermal fracture mechanism of rock under temperature is discussed herein. The results provide a reference for analysing the stability of mine roadways, tunnel chambers and buildings after fire exposure, and they enable design of restoration schemes.

2 Sample preparation and experimental method

2.1 Sample preparation

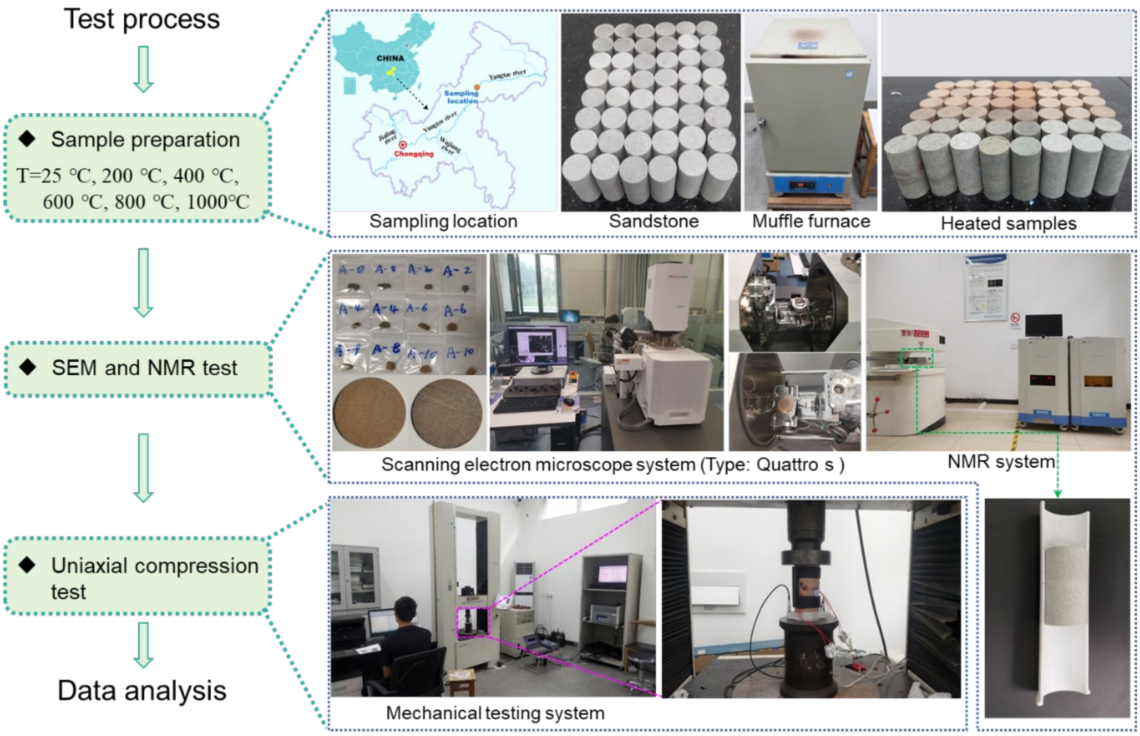

Fig. 1 Samples preparation and test process

This paper takes Chongqing sandstone as the research object. The sandstone is homogeneous in texture, and the main mineral components are quartz, albite, anorthite, calcite and zeolite. In the natural state, the density of the sandstone is 2.35 g/cm^3, the uniaxial compressive strength is 63.5 MPa, the tensile strength is 8.3 MPa, and the deformation modulus is 14.8 GPa. To reduce the influence of sample dispersion on the research results, all samples selected in this study were taken from the same rock block. According to the international standard of rock mechanics (ISRM) recommended standard [30]. A core with a diameter of 50 mm was obtained by drilling, and then the samples without obvious cracks were cut in turn to obtain a cylindrical standard rock sample with a size of φ50 × 100 mm. To control the surface flatness of the sample to within ± 0.02 mm and the parallelism to within ±0.05 mm, all of the samples were polished. Finally, rock samples that met the test requirements were obtained, as shown in Fig. 1.

2.2 Thermal treatment

The box muffle furnace (SX 2 -10-12A) was used to heat the samples at different temperatures, which is produced in Shaoxing, China, with a maximum temperature of 1200 °C. Based on the experimental process, the prepared cylindrical standard rock samples were divided into six groups with three samples in each group. One group was the control group that was not heated, and the other groups were heated at 200, 400, 600, 800 and 1000 °C. After the box muffle furnace reached the set temperature, the samples were kept at the set temperature for 4 h and then cooled to room temperature in a muffle furnace. Finally, sandstone samples treated at different temperatures were obtained, as shown in Fig. 1.

2.3 NMR analysis

In order to analyze the pore distribution characteristics of sandstone samples after different temperatures heated, macromr12-150h nuclear magnetic resonance test system (as shown in Fig. 1) produced by Shanghai Newman Electronic Technology Company was used to test the sandstone samples. The test system consisted of three parts: an NMR magnet, an electronic control system and NMR test software. The main magnetic field intensity was 0.3 T, the probe coil diameter was 150 mm, the RF pulse frequency was 1 ~ 42 MHz, the magnet temperature was 25 ~ 35° and the RF power was 300 W. Before NMR analysis, all samples were saturated with water after vacuum pumping with a ZYB-II vacuum pressure saturation device, and the vacuum pressure was 0.1 MPa. After maintaining vacuum pressure for 4 h, distilled water was injected into the container, and the samples were immersed in distilled water and left standing for 24 h to completely saturate the samples. The NMR test was performed only after the sample was hydrated.

2.4 SEM test

To observe the micromorphology characteristics of sandstone samples after temperature treatment, 6 groups of rock samples with length × width × height of 1 × 1 × 0.5 cm^3 were made. Except for one group of samples used as a control group without temperature treatment, other groups of samples were subjected to 200 °C, 400 °C, 600 °C, 800 °C and 1000 °C. In addition, due to the poor electrical conductivity of sandstone samples, it was necessary to spray gold and paste conductive adhesive on the samples before vacuuming. Finally, the different samples were observed by a Quattro S scanning electron microscope system, and micromorphology photos of each sample were obtained.

3 Test results and analysis

3.1 Pore distribution characteristics of sandstone based on the T_2 spectrum

According to the principles of NMR, the total lateral relaxation rate $\frac{1}{T_2}$ can be expressed as follows:

$$\frac{1}{T_2}=\frac{1}{T_{2b}}+\frac{1}{T_{2s}}+\frac{1}{T_{2d}}, \tag{1}$$

where T_{2b} is the transverse relaxation time of free fluid; T_{2s} is the transverse relaxation time of fluid caused by surface relaxation; and T_{2d} is the transverse relaxation time caused by diffusion relaxation in a gradient magnetic field; surface relaxation plays a major role. Based on Eq. (1), the T_2 spectrum obtained by NMR experiments can reflect the pore size distribution characteristics of sandstone samples treated at different temperatures. The value of T_2 is positively correlated with the size of the aperture; that is, the smaller the value of T_2 is, the smaller the aperture is. The larger the T_2 value, the larger the aperture. The peak value of the T_2 spectrum is positively correlated with the number of pores; that is, the larger the peak value is, the greater the number of pores of the corresponding pore size. Fig. 2 shows the T_2 spectra of the samples after heating at different temperatures. The ordinate represents the cumulative porosity of pores with the corresponding relaxation time. The sum of the ordinates of all data points is the porosity of the sample. According to calculations, the porosities of sandstone samples treated at different temperatures (25~1000 °C) increased gradually with increasing temperature and were 6.81%, 8.08%, 9.36%, 12.73%, 13.91% and 15.62%, respectively.

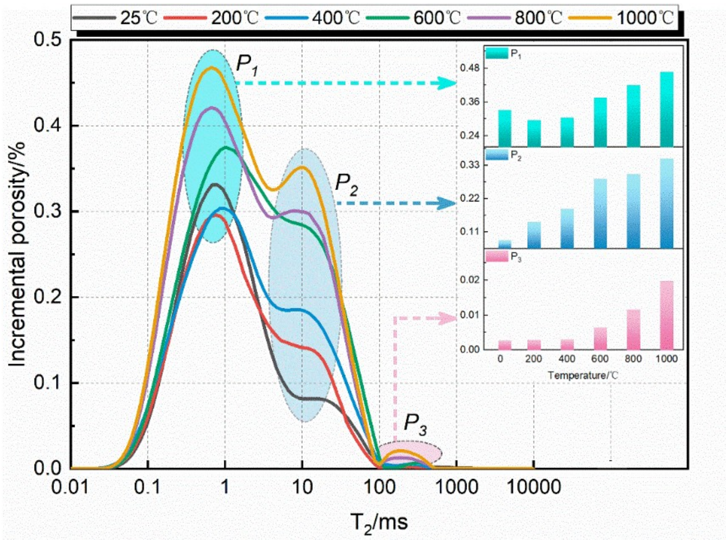

Fig. 2 T_2 spectrum of different samples

It is obvious from Fig. 2 that the T_2 spectra of different samples are composed of three peaks labelled P_1, P_2 and P_3 from left to right, and their corresponding relaxation times were 0.1 ~ 1 ms, 1 ~ 100 ms and 100 ~ 1000 ms, respectively. According to previously published results of pore size division for different relaxation times, the three peaks P_1, P_2 and P_3 can be considered to represent micropores, mesopores and macropores, respectively, indicating that there are a large number of pores with different diameters in the sandstone sample. In addition, the peak point P_1 of the T_2 spectrum of each sample in Fig. 2 is the highest, which indicates that the pores in sandstone samples exist mainly in the form of small pores, and this distribution is independent of temperature. However, by comparing the three peaks of the T_2 spectrum curve of sandstone samples treated with different temperatures, it is obvious that the temperature had a significant effect on the distribution of different pore sizes. The specific analysis is as follows:

(1) After treatment at room temperature (25 °C), the T_2 spectrum curve was mainly composed of the first spectrum peak, in which the peak points P_1, P_2 and P_3 were 0.331%, 0.082% and 0.0025%, respectively, indicating that the pores of sandstone samples treated at room temperature were mainly composed of micropores, and there were a small number of mesopores and a small number of macropores.

(2) When sandstone samples were treated at 200 °C and 400 °C, the first peak value of the T_2 spectrum curve decreased, the second peak value increased, and the third peak value exhibited no significant change compared with that of the room temperature sample. This is because under the influence of temperature, some small holes of sandstone samples are closed due to the extrusion of rock particles after thermal expansion, resulting in a decrease in the P_1 value. However, some particles are staggered due to the extrusion of particles, resulting in an increase in mesopore size pores. Although the number of mesopores increased in the samples treated at 200 °C and 400 °C, the P_3 value did not change significantly compared with the samples treated at ambient temperature, indicating that new pores and cracks of large pore size did not appear at 200 °C and 400 °C. These results further explain the observation of many scholars that when the temperature is kept lower than 400 °C, the strength of the treated sample not only does not decrease significantly in comparison with that of the ambient temperature sample, but it shows some strength enhancement [2, 23].

(3) When the treatment temperature reached 600 °C, compared with the ambient temperature sample, the three peaks of the T_2 spectrum curve increased significantly, among which the peak points P_1, P_2 and P_3 were 0.375%, 0.286% and 0.0071%, respectively, reflecting increases of 13.3%, 248.8% and 184%, respectively. The porosities of sandstone samples changed significantly after treatment at 600 °C, and the porosities of different pore types increased significantly; in particular, mesopores and macropores exhibited substantial increases. This was mainly due to the thermal expansion of rock particles under the influence of temperature, the extrusion of particles leading to cracks, and the thermal stress resulting from different expansion coefficients of particles, which resulted in microcracks between particles. On the other hand, when the temperature exceeded 573 °C, quartz particles changed from the α phase to the β phase, which also caused expansion cracks in the rock particles.

(4) When the samples were treated at 800 °C and 1000 °C, the three peaks of the T_2 spectrum

curve of sandstone samples were larger than those of the samples treated at lower temperatures. Taking 1000 °C as an example, the three peaks of the T_2 spectrum curve were obvious, especially the third peak (P_3), which was not obvious before treatment. After 1000 °C, the P_3 value reached 0.0218%, an increase of 772% compared with the P_3 peak of the ambient temperature sample. In addition, P_1 and P_2 also increased significantly, reaching 0.467% and 0.352%, and the increase rates were 41.1% and 329.3%, respectively, compared with those of the ambient temperature sample. After treatment at 1000 °C, the number of pores in the sandstone increased significantly, especially the mesopores and macropores. These newly formed meso-pores and macropores will directly affect the mechanical properties of rock. This further explains the rapid decline in the mechanical properties of rock after high-temperature treatment.

3.2 Microstructural characteristics of sandstone based on SEM

To analyse the thermal crack characteristics of temperature-treated rocks, rock samples with small sizes (1×1×0.5 cm³) were made, and SEM tests were carried out to obtain microscopic morphology images of each sample, as shown in Fig. 3. After treatment at room temperature (25 °C), the surface of the sandstone sample was uneven, with clear and smooth grain boundaries, and the overall structure was relatively dense, with an obvious step-like structure visible. After treatment at 200 °C (as shown in Fig. 3(b)), the surface of the sample was still uneven, with clear grain boundaries and obvious step-like structures, but pinnate structures appeared, which did not appear in the room temperature sample. This may be due to the evaporation of water on the sample surface after treatment at 200 °C, which causes the flocculent structure material originally close to the sample surface to become fluffy after drying and show a pinnate structure. Other than the differences discussed above, the overall structures of the samples had no obvious changes compared with the structures of the room temperature samples. When the pretreatment temperature reached 400 °C (Fig. 3(c)), the surface of the sample was smooth, the clarity of the particle boundary was obviously reduced, and the colour of the image rock was dim. Unlike the previous sample (treated at 200 ºC), there was an obvious dry area at the edge of the step at this temperature, and the smoothness of the step surface was also significantly reduced. However, the rock surface was intact and without obvious thermal cracks after treatment at 400 °C. When the pretreatment temperature reached 600 °C (as shown in Fig. 3(d)), there was no obvious step-like structure on the rock surface; instead, there was a local layered structure, which had a loose structure, poor contact effect, and obvious microcracks among layered structures. In addition, there were obvious cracks on the surface of the sample, which had not appeared before, and their width was less than 1 μm. The sandstone produced thermal fracture cracks under thermal stress at 600 °C, which exactly explains why the three peaks of the T_2 spectrum curve in Fig. 2 increase significantly for the 600 °C sample compared with the room temperature sample. When the temperature reached 800 °C (as shown in Fig. 3(e)), there were obvious crisscrossing network cracks on the surface of the sample. Due to dissolution and decomposition of particle boundaries after high temperature treatment, the surface of the sample was dark and rough, and no smooth step structure appeared. Under the influence of temperature, the opening of the crack caused by thermal expansion was further increased (the crack width reached 7.9 μm). At the same time, there were many crisscrossing small cracks that connect and run through each other, forming an obvious network crack structure. When the temperature reached 1000 °C (as shown in Fig. 3(f)), the width of the thermal crack on the surface of the sample treated at this temperature increased significantly compared with that at 800 °C, and two main intersecting cracks appeared. The measured widths reached 10.4 μm and 8.8 μm. At the same time, the fine thermal cracks also propagated and penetrated further and finally formed an obvious network structure. After 800 °C and 1000 °C treatment, the cracks of the sample increased significantly, and thermal cracking cracks with larger widths were produced, which further explains the observation that the P_3 value of the T_2 spectrum curves of the samples treated at 800 °C and 1000 °C increased significantly compared with that of the room temperature sample (Fig. 2).

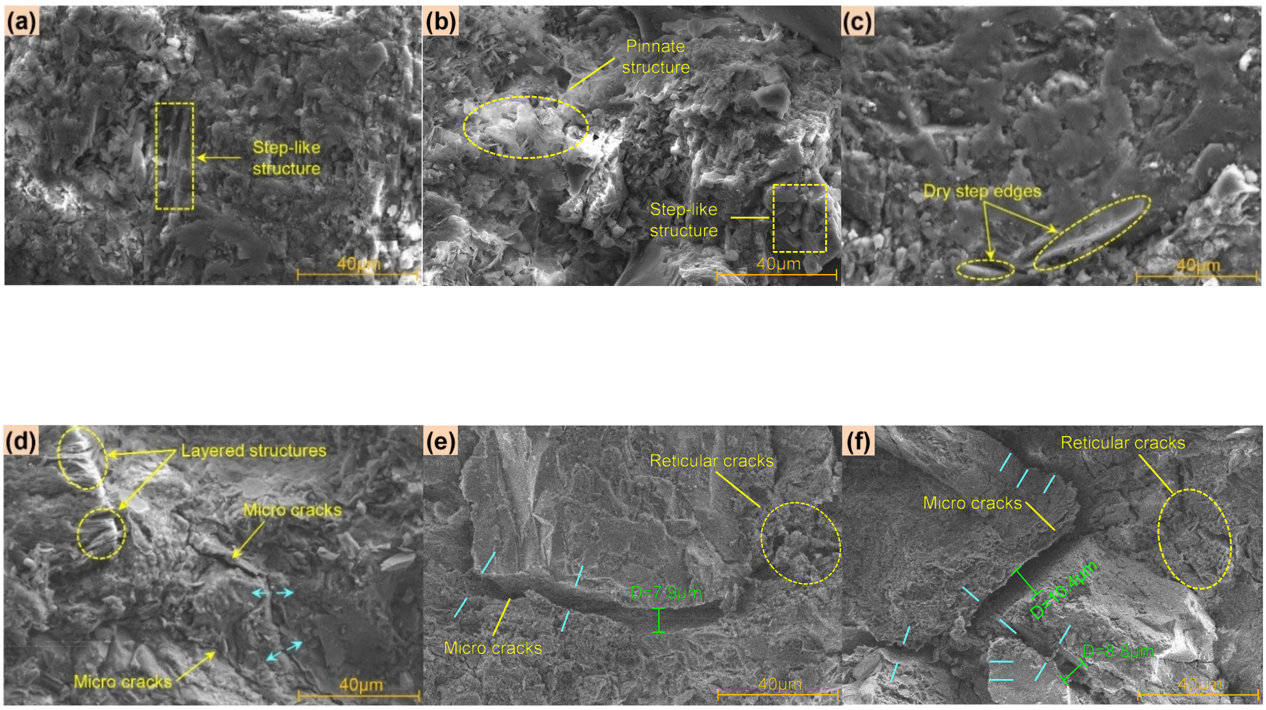

Fig. 3 Micromorphology of sandstone samples treated after different temperatures (×3000): (a) 25℃; (b) 200℃; (c) 400℃; (d) 600℃; (e) 800℃; (f) 1000℃

The above analysis shows that obvious thermal cracks appeared in the rock material after the temperature was raised, especially when the temperature exceeded 400 °C. However, when a rock is subjected to high temperature, the interior rock units are constrained by the surrounding rock mass, while the rock units on the surface of the rock have free faces, which leads to the difference in the thermal cracks of the rocks appearing in different locations. For example, Meng et al.[31] and Li et al.[32] conducted CT tests on coal samples treated at different temperatures ranging from 25 °C to 600 °C and obtained CT images of sections from the middle of the coal samples. Fig. 4 shows typical CT images obtained after heating at 100 °C, 500 °C and 600 °C. As seen from the distribution of thermal cracks, there are two areas in the image, Area A near the centre and Area B near the outer edge. The opening and density of hot cracks in Area A are obviously larger than those in Area B. These results show that the distribution of thermal cracks in coal samples has regional differences. To explore whether there were also regional differences in thermal cracks in the sandstone described in this paper, 5 mm thin sections of rock was extracted from the middle of the cylindrical samples after high-temperature treatment; these were subjected to SEM testing, and the thermal cracking status of different parts of the section were observed, as shown in Fig. 5 (considering that the structure of sandstone is more compact than that of coal, the thermal cracks of sandstone were observed by SEM). Samples treated at 600 °C and 1000 °C were selected for typical analysis. It can be seen from Fig. 5 that because of the central position of the sample, the crack opening and crack density of the rock unit at the edge of the sample increased significantly. These results show that the distribution of thermal cracks is related to the spatial location of the cracks in the rock mass. To further explain this phenomenon from a theoretical point of view, this paper describes theoretical calculations and analyses in section 4.

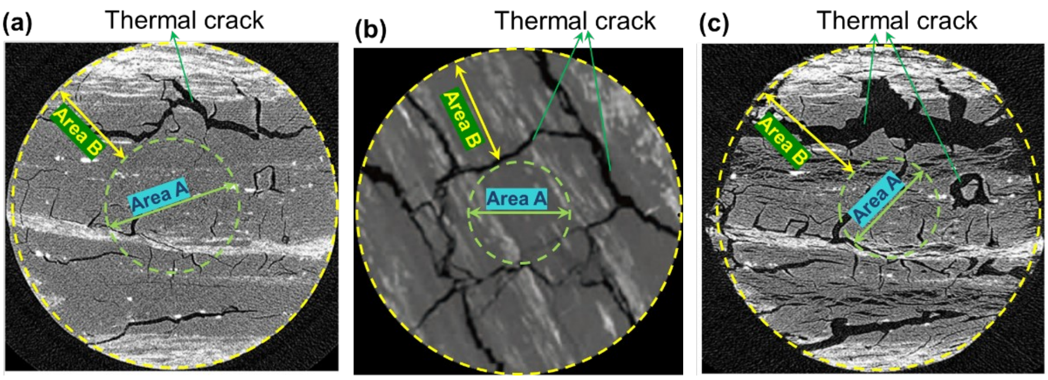

Fig. 4 CT scanning maps of the section in middle of coal sample under different temperatures: (a) 100°C; (b) 500 °C; (c) 600 °C. The sample section can be divided into Area A and Area B according to the characteristics of thermal crack distribution. The thermal crack density and crack opening of Area A near the outer edge of the sample are significantly higher than that of Area B near the center of the sample[31, 32].

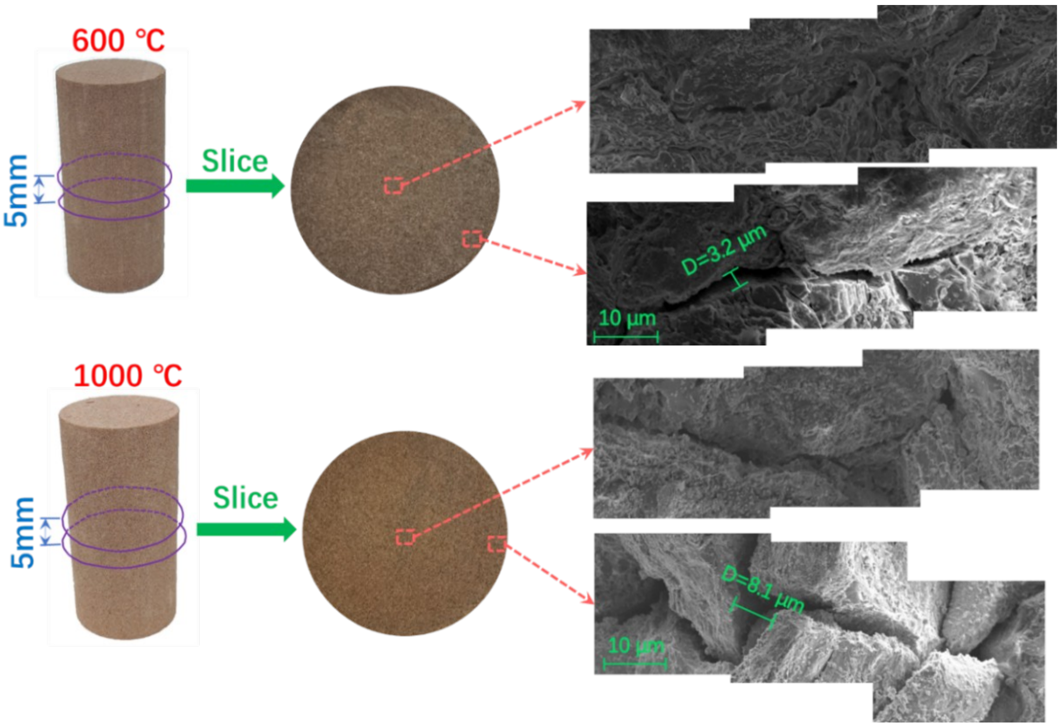

Fig. 5 Microthermal fracture of rock units at different locations

4 Thermal stress mechanics model and thermal fracture mechanism analysis

The NMR and SEM results show that temperature is the main factor affecting the pore structure of rock. To further explore the mechanism of thermal fracture of rock caused by temperature, the corresponding theoretical model was established based on the theory of thermoelasticity and compared, analysed and verified with the experimental results.

4.1 Thermoelastic mechanical model of random media

To establish the mechanical model of rock thermal fracture under the influence of temperature, the theory of elastic mechanics was used to develop the following hypotheses that are described before constructing the theoretical model [33]: 1) Sandstone is composed of random heterogeneous particles at the mesoscale, but it is a homogeneous isotropic elastic medium at the macroscale. 2) The physical and mechanical parameters of sandstone unit particles are the statistical characteristics of many mineral particles. 3) Due to the small size of the sandstone unit in the mesoscale, it does not have macroscopic statistical characteristics, so the mechanical properties of the unit expressed by meso particles show random heterogeneous characteristics on the whole. 4) The elastic modulus, Poisson's ratio, bulk modulus, internal friction angle, cohesion and compressive strength of the sandstone meso unit also have the characteristics of random heterogeneity, and the randomness of all the above parameters is unified.

According to Hypothesis 1) and based on the basic theory of elastoplastic mechanics, the stress balance equation of a rock mass is as follows,

$$\sigma_{ij,j}+F_i=0, \quad (2)$$

By considering the influence of temperature, the stress balance equation of the rock mass under the action of temperature is obtained as follows,

$$\sigma_{ij,j}+F_i-3K\alpha T_{,i}=0, \quad (3)$$

where F_i is the external force, K is the bulk deformation modulus of rock, α is the thermal expansion coefficient of rock, and T is the temperature.

In elasticity, there are the following basic equations,

$$\sigma_{ii}=\lambda\varepsilon+2G\varepsilon_{ii}, \quad (4)$$

$$\tau_{ij}=G\left(u_{i,j}+u_{j,i}\right), \quad (5)$$

$$\varepsilon_{ii}=u_{i,i}, \quad (6)$$

$$\varepsilon=\sum\varepsilon_{ii}, \quad (7)$$

By substituting Eqs. (4) ~ (7) into Eq. (3), and according to Hypothesis (4), the elastoplastic mechanical model of a random heterogeneous rock mass expressed by displacement and considering the effect of temperature can be obtained as follows

$$\left(\lambda+G\right)\frac{\partial\varepsilon}{\partial x_i}+G\nabla^2 u+\frac{\partial\lambda}{\partial x_i}\varepsilon+\sum_{j=1}^{3}\frac{\partial G}{\partial x_j}\frac{\partial u_i}{\partial x_j}+\sum_{j=1}^{3}\frac{\partial G}{\partial x_j}\frac{\partial u_j}{\partial x_i}+F_i=3\left(K\alpha\frac{\partial T}{\partial x_i}+KT\frac{\partial\alpha}{\partial x_i}+\alpha T\frac{\partial K}{\partial x_i}\right), \quad (8)$$

In the process of theoretical analysis, it is assumed that the Lame constants λ and G of the rock are constants; then, Eq. (8) can be modified into

$$\left(\lambda+G\right)\frac{\partial\varepsilon}{\partial x_i}+G\nabla^2 u+F_i=3\left(K\alpha\frac{\partial T}{\partial x_i}+KT\frac{\partial\alpha}{\partial x_i}\right), \quad (9)$$

Eq. (9) is the deformation caused by the temperature gradient and thermal expansion gradient of the rock under the influence of temperature. In other words, it is considered that both the temperature and thermal expansion coefficient of the rock are functions of coordinates. Compared with the traditional thermoelastic model, the deformation term $3KT\frac{\partial\alpha}{\partial x_i}$ caused by the thermal expansion coefficient gradient was not considered in previous studies. Because this part of deformation has a great influence on the total deformation of rock under the influence of temperature, this theoretical model better reflects the characteristics of rock thermal deformation under the influence of temperature.

The rock sample used in this study is a cylindrical standard rock sample, so Eq. (9) needs to be transformed into a polar coordinate equation. The temperature (T) and thermal expansion coefficient (α) are both functions of r and T, and the displacement generated by thermal stress is also denoted as u and v, respectively. Based on this, the polar coordinate equation of the thermoelastic mechanical model of random heterogeneous rock materials can be expressed according to Eq. (9) as

$$\frac{E}{1-\mu^2}\cdot\frac{\partial\varepsilon}{\partial r}-\frac{E}{1+\mu}\cdot\frac{1}{r}\cdot\frac{\partial}{\partial\theta}\left\{\frac{1}{2r}\left[\frac{\partial(rv)}{\partial r}-\frac{\partial u}{\partial\theta}\right]\right\}=\frac{E\alpha}{1-2\mu}\cdot\frac{\partial T}{\partial r}+\frac{ET}{1-2\mu}\cdot\frac{\partial\alpha}{\partial r}, \tag{10}$$

$$\frac{E}{1-\mu^2}\cdot\frac{1}{r}\cdot\frac{\partial\varepsilon}{\partial\theta}-\frac{E}{1+\mu}\cdot\frac{\partial}{\partial r}\left\{\frac{1}{2r}\left[\frac{\partial(rv)}{\partial r}-\frac{\partial u}{\partial\theta}\right]\right\}=\frac{E\alpha}{1-2\mu}\cdot\frac{\partial T}{\partial\theta}+\frac{ET}{1-2\mu}\cdot\frac{\partial\alpha}{\partial\theta}, \tag{11}$$

$$\varepsilon=\varepsilon_r+\varepsilon_\theta, \tag{12}$$

Correspondingly, the constitutive equation of rock is

$$\begin{cases}\sigma_r=\dfrac{E}{1-\mu^2}\left(\dfrac{\partial u}{\partial r}+\dfrac{u}{r}\dfrac{\partial v}{\partial\theta}+\mu\dfrac{u}{r}\right)-\dfrac{E\alpha T}{1-2\mu}\\ \sigma_\theta=\dfrac{E}{1-\mu^2}\left(\dfrac{1}{r}\dfrac{\partial v}{\partial\theta}+\dfrac{u}{r}+\mu\dfrac{\partial u}{\partial r}\right)-\dfrac{E\alpha T}{1-2\mu}\\ \tau_{r\theta}=\dfrac{E}{2(1+\mu)}\left(\dfrac{\partial v}{\partial\theta}+\dfrac{1}{r}\dfrac{\partial u}{\partial\theta}-\dfrac{v}{r}\right)-\dfrac{E\alpha T}{1-2\mu}\end{cases}, \tag{13}$$

where E is Young's modulus, μ is Poisson's ratio, u and v are displacements, respectively, and T and α are the temperature and thermal expansion coefficients related to r and θ, respectively. However, in the case of plane stress for an axisymmetric problem, the temperature and thermal expansion coefficients of the sample during the heating process are independent of θ and are only functions of r, so $T=T(r)$ and $\alpha=\alpha(r)$. At the same time, their displacement must also be axisymmetric, i.e., $u=u(r)$ and $v=0$. Clearly, Eq. (11) is always true, and Eq. (10) can be rewritten as follows,

$$\frac{\partial}{\partial r}\left(\frac{\partial u}{\partial r}+\frac{u}{r}\right)=\alpha\frac{1-\mu^2}{1-2\mu}\cdot\frac{\partial T}{\partial r}+T\frac{1-\mu^2}{1-2\mu}\cdot\frac{\partial\alpha}{\partial r}, \tag{14}$$

After integrating both sides of Eq. (14), $u(r)$ can be obtained as follows,

$$u(r)=\frac{1-\mu^2}{r(1-2\mu)}\int_0^r r\alpha(r)T\,dr+C_1 r+C_2\frac{1}{r}, \tag{15}$$

where C_1 and C_2 are integral constants, which can be obtained from given boundary conditions, and $\alpha(r)$ is the random variable of the rock expansion coefficient that changes with r under the influence of temperature, which can be analyzed according to probability statistical theory. Based on the Weibull distribution theory, the thermal expansion coefficient is analysed, and the distribution characteristics of the thermal stress of rock are discussed. Therefore, the distribution function of the thermal expansion coefficient $\alpha(r)$ is

$$F(r)=1-e^{-\left(\frac{\alpha(r)}{\alpha_0}\right)^m}, \tag{16}$$

Eq. (16) can be further modified into

$$\alpha(r)=\alpha_0\left[-\ln\left(1-F(r)\right)\right]^{m^{-1}},\ (r>0)\ , \tag{17}$$

where α_0 is the homogeneity of the expansion coefficient of the rock sample; m is the distribution parameter; and $F(r)$ is a function based on the Weibull distribution, with $0<F(r)<1$. According to Weibull distribution theory, the curve of the $F(r)$ function increases monotonically. Additionally, compared with the hyperbolic tangent function H(x), both of them have the same changing trend. The expression of the H(x) function is shown in Eq. (18). Therefore, to obtain the thermal expansion coefficient $\alpha(r)$, the hyperbolic tangent function H(x) can be introduced into Eq. (17). Combined with Eqs. (17) and (18), the equation for calculation of the thermal expansion coefficient $\alpha(r)$ of the sample can be obtained as in Eq. (19).

$$H(x)=\tanh(mx)=\frac{e^{mx}-e^{-mx}}{e^{mx}+e^{-mx}},\ (x>0)\ , \tag{18}$$

$$\alpha(r)=\alpha_0\left[-\ln\left(1-\frac{e^{mr}-e^{-mr}}{e^{mr}+e^{-mr}}\right)\right]^{m^{-1}}, \tag{19}$$

Combining Eqs. (13), (15) and (19), the thermal stress of the plane stress problem can be obtained as follows,

$$\sigma_r=\frac{-E(1-\mu)}{(1-2\mu)r^2}\int_0^r r\alpha(r)T(r)dr+\frac{C_1E}{1-\mu}-\frac{C_2E}{(1-\mu)r^2}, \tag{20}$$

$$\sigma_\theta=\frac{E(1-\mu)}{(1-2\mu)r^2}\int_0^r r\alpha(r)T(r)dr-E\alpha(r)T(r)+\frac{C_1E}{1-\mu}-\frac{C_2E}{(1-\mu)r^2}, \tag{21}$$

$$\tau_{r\theta}=0, \tag{22}$$

For the plane strain problem, $\acute{E}=\frac{E}{1-\mu^2}$, $\acute{\mu}=\frac{\mu}{1-\mu}$ and $\acute{\alpha}(r)=(1+\mu)\alpha(r)$ can replace E, μ and $\alpha(r)$, respectively, in Eq. (21), so the thermal stress in the plane strain problem can be described as follows,

$$\sigma_r=\frac{-E(1-2\mu)}{(1-\mu)(1-3\mu)r^2}\int_0^r r\alpha(r)T(r)dr+\frac{C_1E}{(1+\mu)(1-2\mu)}-\frac{C_2E}{(1+\mu)(1-2\mu)r^2}, \tag{23}$$

$$\sigma_\theta=\frac{E(1-2\mu)}{(1-\mu)(1-3\mu)r^2}\int_0^r r\alpha(r)T(r)dr-\frac{E}{1-\mu}\alpha(r)T(r)+\frac{C_1E}{(1+\mu)(1-2\mu)}-\frac{C_2E}{(1+\mu)(1-2\mu)r^2}, \tag{24}$$

$$\tau_{r\theta}=0, \tag{25}$$

4.2 Thermal stress distribution of samples

The size of the solid cylindrical standard rock sample selected in this study is φ50 × 100 mm (R=0.0025 m). When the sample was not heated, there are the following boundary conditions under the condition that there is no external force on the boundary: 1) when $r=0$, $\sigma_r=0$ and 2) when $r=R$, $\sigma_r=0$. By substituting these boundary conditions into Eqs. (23) and (24), the integral constants C_1 and C_2 can be obtained as follows,

$$\begin{cases} C_1=\dfrac{(1-2\mu)^2(1+\mu)}{(1-\mu)(1-3\mu)R^2}\displaystyle\int_0^R r\alpha(r)T(r)\,dr \\ C_2=0 \end{cases}, \tag{26}$$

By substituting Eq. (26) into Eqs. (23) and (24), the thermal stress in the cylindrical specimen can be obtained as follows,

$$\sigma_r=\frac{-E(1-2\mu)}{(1-\mu)(1-3\mu)r^2}\left\{\int_0^r r\alpha(r)T(r)\,dr\right\}+\frac{E(1-2\mu)}{(1-\mu)(1-3\mu)R^2}\int_0^R rT(r)\alpha(r)\,dr, \tag{27}$$

$$\sigma_\theta=\frac{E(1-2\mu)}{(1-\mu)(1-3\mu)r^2}\left\{\int_0^r r\alpha(r)T(r)\,dr\right\}-\frac{E}{1-\mu}\beta(r)T(r)+\frac{E(1-2\mu)}{(1-\mu)(1-3\mu)R^2}\int_0^R rT(r)\alpha(r)\,dr, \tag{28}$$

The distribution parameter of the Weibull distribution is 5. The average thermal expansion coefficient α_0 of sandstone samples is 1.5×10^{-5}/°C. The deformation modulus of sandstone is 14.8 GPa, and the Poisson's ratio is 0.23. According to Kang Jian's results [33], the temperature distribution function inside the rock sample during the heating process is given as follows,

$$T(r)=T_0+(T_a-T_0)\left(\frac{r}{R}\right)^2, \tag{29}$$

where T_0 is the centre temperature of the sample at room temperature in °C; T_a is the target temperature of the sample in °C; and R is the radius of the sandstone sample in m. By substituting Eq. (29) into Eqs. (27) and (28), respectively, the theoretical values of radial and circumferential thermal stresses (σ_r and σ_θ) inside random heterogeneous sandstone samples can be calculated based on the Weibull distribution at different temperatures. The three-dimensional surface diagrams of radial and circumferential thermal stresses are shown in Fig. 6 and Fig. 7.

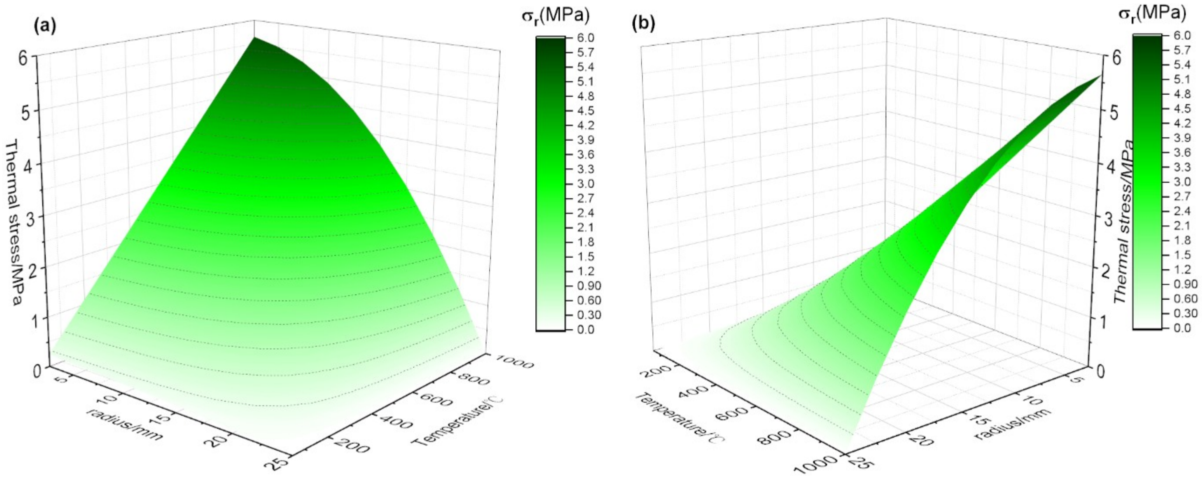

Fig. 6 3D surface diagram of the radial thermal stress of rock: (a) front view; (b) right view. Note: a positive number indicates compressive stress, and a negative number indicates tensile stress.

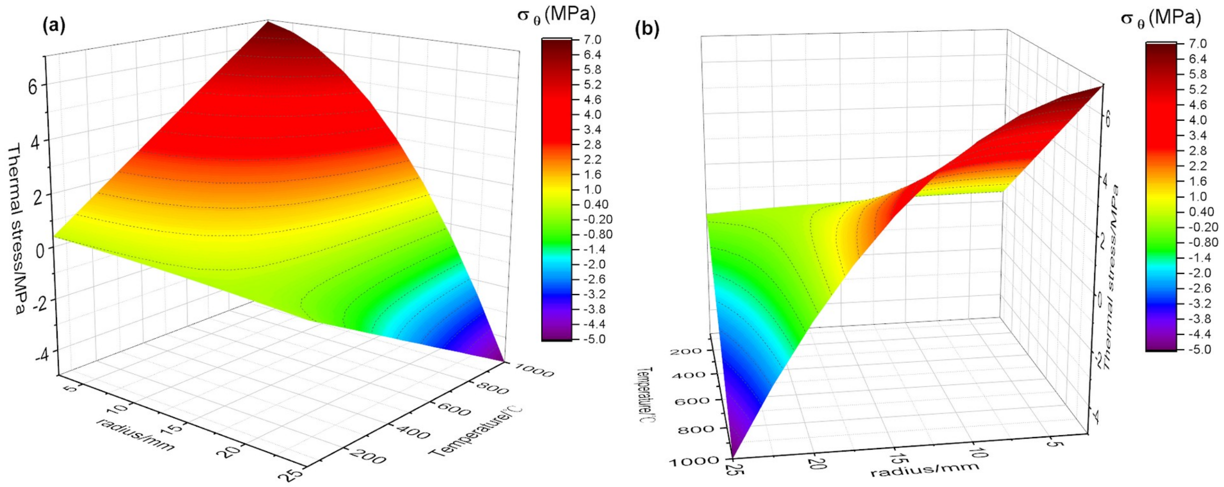

Fig. 7 3D surface diagram of circumferential thermal stress of rock:(a) Front view; (b) Right view

4.3 Thermal fracture mechanism analysis of cylindrical sandstone samples

It can be seen from Fig. 6 and Fig. 7 that the specific analysis of radial thermal stress σ_r and circumferential thermal stress σ_θ calculated according to the theoretical model is as follows:

First, for the radial thermal stress σ_r, as shown in Fig. 6, the thermal stress of rock at different temperatures mainly comprises compressive stress. When the radius decreases and the temperature rises, the compressive stress increases. The main results are as follows: when the temperature is 25 °C, the radial thermal stress inside the sample is 0. With increasing temperature, the radial thermal stress at the centre of the specimen gradually increases. At a given temperature, the radial thermal stress σ_r gradually decreases with increasing radius until it reaches the outer edge of the specimen and drops to 0. This indicates that the radial thermal stress inside the sandstone under the influence of temperature causes the rock particles to squeeze each other along the radius direction, and the closer they are to the centre, the more obvious is the squeezing effect. In contrast, the closer a location is to the outer edge of the specimen, the weaker the extrusion effect. This is because the rock is in a state with no external force in the heating process, so the sample can expand freely along the direction of the wall under the action of temperature. However, during the expansion of the rock unit, an internal unit of the sample is squeezed by the surrounding particles and produces compressive stress, while a rock unit at the outer edge comprises the free surface, so the radial extrusion force cannot be produced on the outer surface of the unit.

Second, in considering the circumferential thermal stress σ_θ due to the influence of temperature, Fig. 7 shows that the circumferential thermal stress exhibits compressive stress near the axis and tensile stress near the outer edge of the sample, and the higher the temperature is, the more obvious this trend. For example, when the temperature is 200 °C, σ_θ = 1.42 MPa at the centre of the sample (r = 0), which indicates compressive stress, and σ_θ = - 0.79 MPa at the outer edge of the sample (r = 25 mm), which indicates tensile stress. When the temperature reaches 1000 °C, σ_θ = 6.95 MPa at the centre of the sample (r = 0), showing compressive stress, and σ_θ= - 5.01 MPa at the outer edge of the sample (r = 25 mm), showing obvious tensile stress. The above results show that the circumferential thermal stress σ_θ of rock shows the two stress modes compression and tension, which differs from the radial thermal stress σ_r; with increasing temperature, the compressive stress at the centre and the tensile stress at the outer edge of the sample increase gradually.

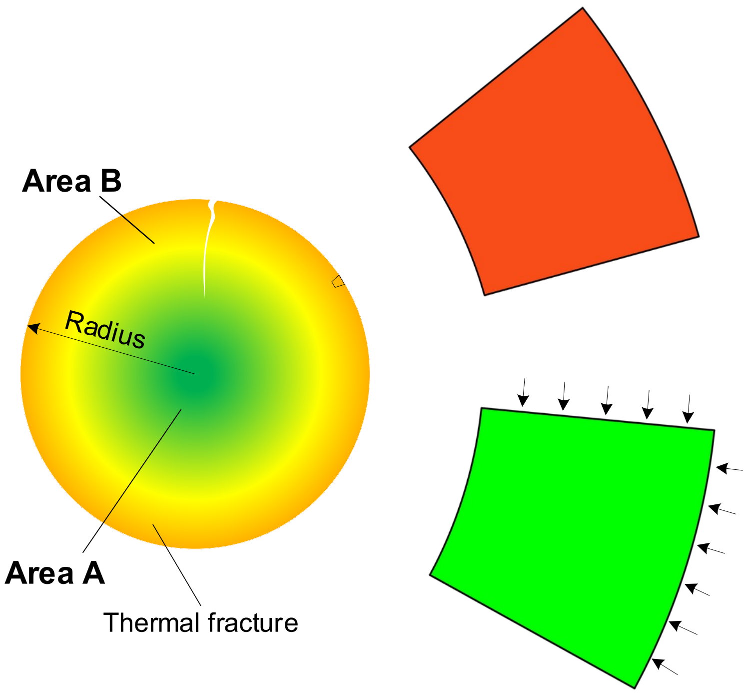

Fig. 8 Schematic diagram of stress on rock units at different positions of the sample

It can be seen from the above analysis that the theoretical value of thermal stress calculated by the mechanical model constructed in this study would cause the rock particles to squeeze each other near the centre of the sample, and the tensile stress between the rock particles would gradually increase near the outer edge due to the gradual enhancement of circumferential tensile stress. As rock is a natural medium with initial void fractures, rock units at different locations will experience different stress processes under the above thermal stress, as shown in Fig. 8. In area A near the centre, the rock particles are subjected to both radial and circumferential compressive stresses, resulting in the mutual compression of particles and the reduction of pores between particles. However, according to Fig. (5), both the circumferential stress and the radial stress are in the range of 0 ~ 7 MPa, which are small compared with the compressive strength of rock. Therefore, the influence of the extrusion between particles on the mechanical properties of rock can be ignored, but mutual extrusion can enhance the effects of contact between particles [22]. Compared with area A near the centre, area B near the outer edge obviously differs. In area B, the radial compressive stress decreases with increasing radius, but the circumferential tensile stress increases, and the higher the temperature is, the greater the circumferential tensile stress in area B. Taking 1000 °C as an example, according to Fig. 7, when the temperature reaches 1000 °C, σ_θ at the outer edge of the sample reaches -5.01 MPa. Because rock is a brittle material, tensile strength is usually very small compared with compressive strength, and under the influence of high temperature, the cement between rock particles gradually decomposes, resulting in obvious weakening of the connection between particles [34, 35]. This will directly weaken the mechanical properties of the rock and even cause the rock particles to displace under the action of circumferential tensile stress; that is, obvious thermal cracks appear on the surface of the sample, as shown in Fig. 8, which further explains the regional differences in the thermal crack distribution in coal and sandstone in Fig. 5.

5 Discussion on the influence of temperature on the macrostrength of rock

According to the analysis in Section 4.3, thermal fracture of cylindrical rock samples under the influence of temperature is mainly related to temperature and the spatial position inside the sample. That is, a rock unit at the centre of the sample is in a state of compression due to the action of circumferential thermal stress and radial thermal stress, while a rock unit at the outer edge of the sample is in a state of tension due to the tensile action of circumferential thermal stress. Because rock exhibits pressure resistance but not tensile resistance, an overly high temperature will cause formation of many thermal cracks in the rock due to the action of thermal stress; this will then decrease the mechanical properties of the rock. Therefore, the change in the internal pore size of the sample is small when the temperature is between 25 °C and 400 °C. When the temperature exceeds 600 °C, the number of micropores, mesopores and macropores in the sample increases significantly, and substantial numbers of microthermal cracks appear in the rock at temperatures of 800 °C and 1000 °C, as shown in Fig. 2. Many studies have shown that temperature is an important factor affecting the mechanical properties of rock [36-38]. Therefore, to compare the strength of sandstone after different temperature treatments, uniaxial compression tests were carried out on the samples, and the stress-strain curves of each sample are shown in Fig. 9.

Fig. 9 shows that when the temperature was in the range of 25-400 °C, the peak stress of rock increased gradually with increasing temperature. When the temperature reached 600 °C, the peak stress of rock decreased rapidly with increasing temperature. Especially when the temperature was 1000 °C, the average peak stress of the sample was 32.23 MPa, which is 50.1% lower than that of the ambient temperature sample. This shows that the effect of temperature within a certain range strengthened the mechanical properties of rock, and the mechanical properties of rock deteriorated rapidly when the temperature exceeded that range. From the research of this paper, we can see that the reasons for this phenomenon are as follows:

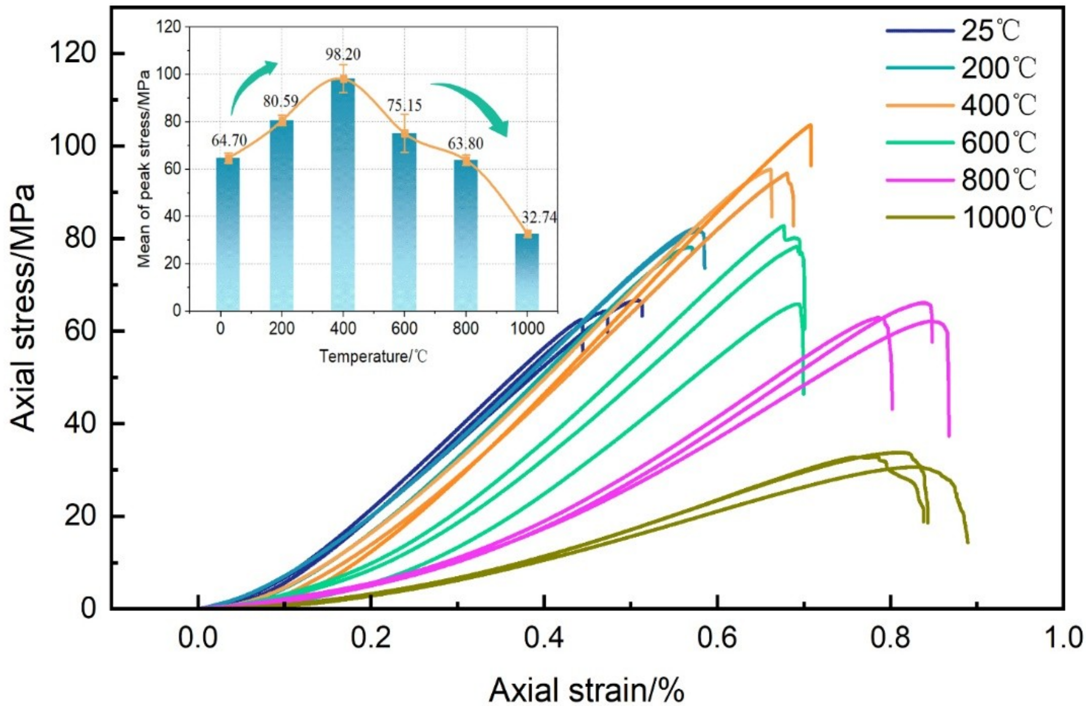

Fig. 9 Stress-strain curves of sandstone samples treated at different temperatures

(1) When the temperature is between 25 and 400 °C, compressive stress is generated at the centre of the sample under the influence of temperature, and tensile stress is generated at the outer edge. According to the calculations of the rock thermal stress mechanics model (as shown in Fig. 8), the σ_r and σ_θ stresses are not more than 2.5 MPa, which is far less than the compressive strength and

tensile strength of rock. Therefore, the mechanical properties of rock are not reduced due to cracks caused by thermal stress. In contrast, the contact effect between rock particles is further enhanced due to water evaporation and mutual extrusion of rock particles under the action of thermal stress, and finally, the peak stress of rock will gradually increase with increasing temperature.

(2) When the temperature reaches 600 °C, on the one hand, quartz transforms from the α phase to the β phase [39], which weakens the contact between rock particles; on the other hand, the mineral composition and cementitious matter of rock gradually decompose under the influence of temperature, the connection between rock particles is more fragile, and the mechanical properties of rock samples gradually deteriorate due to the combined effect of these two influences. However, it can be seen from Fig. 6 and Fig. 7 that the radial thermal stress and circumferential thermal stress of the rock sample increase gradually as the temperature rises, so the thermal cracking of the rock finally increases with increasing temperature due to the effect of thermal stress. Especially when the temperature reaches 1000 °C, larger pore sizes (as shown in Fig. 2) and wider and denser thermal cracks (as shown in Fig. 3) appear in the rock samples. All these factors cause the mechanical properties of rock to deteriorate rapidly under the influence of increased temperatures.

The above analysis shows that although the porosity of sandstone continues to increase with increasing temperature and the macropores and mesopores also gradually increase, this does not mean that all temperatures will cause thermal damage and affect the macromechanical properties of the rock. Thermal stress can enhance the contact between rock particles to a certain extent, and the strength of rock gradually increases in the range 25 ~ 400 °C, which is the most intuitive embodiment. However, the higher temperature will, on the one hand, cause the decomposition of rock minerals and convert the α-β phases of quartz particles; on the other hand, it will also produce greater thermal stress, which will directly cause serious thermal damage to the rock. Therefore, when the temperature exceeds 600 °C, the rock strength decreases gradually with increasing temperature. Therefore, in the repair and reconstruction work done after a fire in a mine roadway, tunnel chamber or building site, the temperature of the fire site should be evaluated scientifically and reasonably according to the type of combustible material involved, and the stability of the engineering rock mass should be evaluated on the basis of the predicted temperature; this will lead to a safer, more reasonable and effective design and construction scheme.

6 Conclusions

In this paper, laboratory experiments and theoretical analysis were combined to study the pore size distributions of sandstone samples subjected to different temperatures, and a thermodynamic model of random heterogeneous rock was constructed. Using the theoretical results, a mechanism for thermal fracture in heated rock was developed. Some important conclusions are as follows:

(1) The T_2 spectra of sandstone samples treated at different temperatures all contained three peaks, indicating that the voids of the samples were composed of small pores, medium pores and large pores. However, with increasing temperature, the porosity of the rock sample increased gradually. The proportion of micropores decreased slightly in the range of 25-400 °C and then increased significantly when the temperature exceeded 600 °C, while the proportion of mesopores and macropores increased continuously with increasing temperature.

(2) When the temperature was between 25 ~ 400 °C, the surface structure of the sample after high temperature treatment was complete, and there was no obvious heat loss crack. When the temperature reached 600 °C, the surface cracks initiated gradually under the influence of temperature and increased with increasing temperature. The widths of thermal cracks reached 10.4 μm at 1000 °C. In addition, the distribution of thermal cracks exhibited regional differences; that is, the thermal crack density and opening of Area A near the centre were obviously lower than those of Area B near the edge of the sample.

(3) By considering the stochastic heterogeneity of the meso unit expansion coefficient of sandstone, a stochastic heterogeneous rock thermal stress mechanical model based on the Weibull distribution was established. The thermal stress distribution characteristics of cylindrical sandstone samples under different temperature treatments were obtained. The theoretical results showed that the radial thermal stress σ_r and circumferential thermal stress σ_θ caused by temperature compressed the rock units near the centre, the rock particles near the outer edge experienced tension, and the tensile stress caused by circumferential thermal stress σ_θ was the main factor causing rock thermal cracking.

(4) Although the porosity of sandstone continued to increase with increasing temperature and the numbers of macropores and mesopores also gradually increased, this does not mean that all temperatures will cause thermal damage to the rock and affect the macromechanical properties of the rock. The peak strength of rock gradually increases with increasing temperature in the range of 25 ~ 400 °C and will not decrease with increasing temperature until the temperature exceeds 400 °C.

Acknowledgements: This work was supported by the National Major Science and Technology Projects of China (Grant numbers 2016ZX05045-004), the National Natural Science Foundation of China (Grant numbers 51874053) and the Fundamental Research Funds for the Central Universities (Grant numbers 2020CDCGJ041)

Conflict of Interest: No conflict of interest exits in the submission of this manuscript, and manuscript is approved by all authors for publication.

Author contributions: Weijing Xiao and Dongming Zhang conceived and designed the experiments; Guo Yu and Haitao Li performed the experiments; Shujian Li, Beichen Yu and Dongwei Li analyzed the data; and Dongming Zhang, Weijing Xiao wrote the paper.

Reference

1. Su Y, Su Y, Zhao M, Vlachopoulos N. Tunnel Stability Analysis in Weak Rocks Using the Convergence Confinement Method. *Rock Mech Rock Eng*. 2020.
2. Xiao W, Zhang D, Wang X. Experimental study on progressive failure process and permeability characteristics of red sandstone under seepage pressure. *Eng Geol*. 2020;265(105406).
3. Cheng H, Zhou X, Pan X, Berto F. Damage analysis of sandstone during the creep stage under the different levels of uniaxial stress using NMR measurements. *Fatigue Fract Eng M*. 2021;44(3):719-732.
4. Lei R, Zhang Z, Ge Z, Berto F, Wang G, Zhou L. Deformation localization and cracking processes of sandstone containing two flaws of different geometric arrangements. *Fatigue Fract Eng M*. 2020;43(9):1959-1977.
5. Washburn TW, Turner PJ, Durden JM, Jones DOB, Weaver P, Van Dover CL. Ecological risk assessment for deep-sea mining. *Ocean Coast Manage*. 2019;176:24-39.
6. Chen S, Yang C, Wang G. Evolution of thermal damage and permeability of Beishan granite. *Appl Therm Eng*. 2017;110:1533-1542.
7. Shaw, George H. Disposal of high-level nuclear waste. *Geology*. 1986;14(5):371.
8. Wasantha PLP, Guerrieri M, Xu T. Effects of tunnel fires on the mechanical behaviour of rocks in the vicinity - A review. *Tunn Undergr Sp Tech.* 2021;108(103667).
9. Akbarzadeh H, Chalaturnyk RJ. Structural changes in coal at elevated temperature pertinent to underground coal gasification: A review. *Int J Coal Geol.* 2014;131:126-146.
10. Chen Y, Hu S, Wei K, Hu R, Zhou C, Jing L. Experimental characterization and micromechanical modeling of damage-induced permeability variation in Beishan granite. *Int J Rock Mech Min*. 2014;71:64-76.
11. Souley M, Homand F, Pepa S, Hoxha D. Damage-induced permeability changes in granite: a case example at the URL in Canada. *Int J Rock Mech Min*. 2001;38(2):297-310.
12. Wu Z, Li M, Weng L. Thermal-Stress-Aperture Coupled Model for Analyzing the Thermal Failure of Fractured Rock Mass. *Int J Geomech*. 2020;20(0402017610).

13. Ma X, Wang G, Hu D, Liu Y, Zhou H, Liu F. Mechanical properties of granite under real-time high temperature and three-dimensional stress. *Int J Rock Mech Min*. 2020;136(104521).
14. Shen Y, Hou X, Yuan J, Wang S, Zhao C. Thermal cracking characteristics of high-temperature granite suffering from different cooling shocks. *Int J Fracture*. 2020;225(2):153-168.
15. Qin Y, Tian H, Xu N, Chen Y. Physical and Mechanical Properties of Granite After High-Temperature Treatment. *Rock Mech Rock Eng*. 2020;53(1):305-322.
16. Xiao W, Zhang D, Yang H, Li X, Ye M, Li S. Laboratory investigation of the temperature influence on the mechanical properties and fracture crack distribution of rock under uniaxial compression test. *B Eng Geol Environ*. 2021;80(2):1585-1598.
17. Zhou, X., Fu, L., Cheng, H., Berto, F. Cracking behaviours of rock−like materials containing three preexisting flaws after high−temperature treatments. *Fatigue Fract Eng M*. 2020; 44(3): 622-635.
18. Ranjith PG, Viete DR, Chen BJ, Perera MSA. Transformation plasticity and the effect of temperature on the mechanical behaviour of Hawkesbury sandstone at atmospheric pressure. *Eng Geol*. 2012;151:120-127.
19. Zhu T, Jing H, Su H, Yin Q, Du Mingrui, Han G. Physical and mechanical properties of sandstone containing a single fissure after exposure to high temperatures. *Int. J. Min. Sci. Technol.* 2016;26(2):319-325.
20. Gautam PK, Verma AK, Jha MK, Sarkar K, Singh TN, Bajpai RK. Study of Strain Rate and Thermal Damage of Dholpur Sandstone at Elevated Temperature. *Rock Mech Rock Eng*. 2016;49(9):3805-3815.
21. Rao Q, Wang Z, Xie H, Xie Q. Experimental study of mechanical properties of sandstone at high temperature. *J. Cent. South Univ.* 2007;141:478-483.
22. Sha S, Rong G, Peng J, Li B, Wu Z. Effect of Open-Fire-Induced Damage on Brazilian Tensile Strength and Microstructure of Granite. *Rock Mech Rock Eng*. 2019;52(11):4189-4202.
23. Wong LNY, Zhang Y, Wu Z. Rock strengthening or weakening upon heating in the mild temperature range? *Eng Geol*. 2020;272(105619):105619.
24. Zhang Y, Sun Q, He H, Cao L, Zhang W, Wang B. Pore characteristics and mechanical properties of sandstone under the influence of temperature. *Appl Therm Eng*. 2017;113:537-543.
25. Tripathi A, Gupta N, Singh AK, Mohanty SP, Rai N, Pain A. Effects of Elevated Temperatures

on the Microstructural, Physico-Mechanical and Elastic Properties of Barakar Sandstone: A Study from One of the World's Largest Underground Coalmine Fire Region, Jharia, India. *Rock Mech Rock Eng*. 2021.

26. Jin P, Hu Y, Shao J, Liu Z, Feng G, Song S. Influence of Temperature on the Structure of Pore-Fracture of Sandstone. *Rock Mech Rock Eng*. 2020;53(1):1-12.
27. Yang S, Tian W, Elsworth D, Wang J, Fan L. An Experimental Study of Effect of High Temperature on the Permeability Evolution and Failure Response of Granite Under Triaxial Compression. *Rock Mech Rock Eng*. 2020;53(10SI):4403-4427.
28. Yin Q, Jing H, Liu R, Su H, Yu L, Han G. Pore characteristics and nonlinear flow behaviors of granite exposed to high temperature. *B Eng Geol Environ*. 2020;79(3):1239-1257.
29. Wang F, Fruehwirt T, Konietzky H, Zhu Q. Thermo-mechanical behaviour of granite during high-speed heating. *Eng Geol*. 2019;260(105258).
30. Fairhurst CE, Hudson JA. Draft ISRM suggested method for the complete stress-strain curve for intact rock in uniaxial compression. *Int J Rock Mech Min*. 1999;36(3):281-289.
31. Meng Q, Zhao Y, Yu Y, Hu Y. Micro-ct experimental study of crack evolution of lignite under different temperatures. *Chn J Rock Mech Eng.* 2010;29(12):2475-2483.
32. LI J, Xue C, Han Q. Study on fracture evolution characteristics of coal rock at different thermal fracture temperatures. *Saf Coal Min*. 2020; 51(1): 22-25,29.
33. Kang J. *Research on thermal cracking of rocks and its application*.: Da Lian University of Technology Press; 2008.
34. Vidana Pathiranagei S, Gratchev I. Engineering properties of sandstone heated to a range of high temperatures. *B Eng Geol Environ*. 2021;80(3):2415-2432.
35. Rathnaweera TD, Ranjith PG, Gu X, et al. Experimental investigation of thermomechanical behaviour of clay-rich sandstone at extreme temperatures followed by cooling treatments. *Int J Rock Mech Min*. 2018;107:208-223.
36. Huang Y, Yang S, Bu Y. Effect of thermal shock on the strength and fracture behavior of pre-flawed granite specimens under uniaxial compression. *Theor Appl Fract Mec*. 2020;106(102474).
37. Li C, Hu Y, Meng T, Jin P, Zhao Z, Zhang C. Experimental study of the influence of

temperature and cooling method on mechanical properties of granite: Implication for geothermal mining. *Energy Sci Eng*. 2020;8(5):1716-1728.

38. Yin T, Li Q, Li X. Experimental investigation on mode I fracture characteristics of granite after cyclic heating and cooling treatments. *Eng Fract Mech*. 2019;222(106740).
39. Shen Y, Yang Y, Yang G, et al. Damage characteristics and thermo-physical properties changes of limestone and sandstone during thermal treatment from-30 degrees C to 1000 degrees C. *Heat Mass Transfer*. 2018;54(11):3389-3407.